Article ID: WMC004374 ISSN 2046-1690

Cell-Free Layer (CFL) Analysis in a Polydimethysiloxane (PDMS) Microchannel: a Global Approach

Corresponding Author:
Mr. Elmano Pinto,
Research fellow, Mechanics department, Polytechnic Institute of Braganca - Portugal

Submitting Author:
Mr. Elmano Pinto,
Research fellow, Mechanics department, Polytechnic Institute of Braganca - Portugal

Other Authors:
Ms. Bruna Taboada,
Research fellow, Mechanics department, ESTiG, Polytechnic Institute of Braganca - Portugal
Ms. Raquel Rodrigues,
Research fellow, Mechanics department, ESTiG, Polytechnic Institute of Braganca - Portugal
Ms. Vera Faustino,
Research fellow, Mechanics department, ESTiG, Polytechnic Institute of BraganÃ§a - Portugal
Dr. Ana Pereira,
Professor, Mathematics department, ESTiG, Polytechnic Institute of Braganca - Portugal
Dr. Rui Lima,
Professor, Mechanics department, Polytechnic Institute of Braganca - Portugal

Article ID: WMC004374

Article Type: Research articles

Submitted on:21-Aug-2013, 01:07:34 PM GMT **Published on:** 21-Aug-2013, 02:35:17 PM GMT

Article URL: http://www.webmedcentral.com/article_view/4374

Subject Categories:BIOMEDICAL ENGINEERING

Keywords: Red blood cells, Blood flow, Cell free layer, Xurography, Nonlinear Optimization, Global Optimization.

How to cite the article: Pinto E, Taboada B, Rodrigues R, Faustino V, Pereira A, Lima R. Cell-Free Layer (CFL) Analysis in a Polydimethysiloxane (PDMS) Microchannel: a Global Approach. WebmedCentral BIOMEDICAL ENGINEERING 2013;4(8):WMC004374

Copyright: This is an open-access article distributed under the terms of the Creative Commons Attribution License(CC-BY), which permits unrestricted use, distribution, and reproduction in any medium, provided the original author and source are credited.

Source(s) of Funding:

This work was supported by: PTDC/SAU-BEB/108728/2008, PTDC/SAU-BEB/105650/2008, and PTDC/SAU-ENB/116929/2010 from FCT (Science and Technology Foundation), COMPETE, QREN and European Union (FEDER).

Cell-Free Layer (CFL) Analysis in a Polydimethysiloxane (PDMS) Microchannel: a Global Approach

Author(s): Pinto E, Taboada B, Rodrigues R, Faustino V, Pereira A, Lima R

Abstract

The cell-free layer (CFL) is a hemodynamic phenomenon that has an important contribution to the rheological properties of blood flowing in microvessels. The present work aims to find the closest function describing RBCs flowing around the cell depleted layer in a polydimethysiloxane (PDMS) microchannel with a diverging and a converging bifurcation. The flow behavior of the CFL was investigated by using a high-speed video microscopy system where special attention was devoted to its behavior before the bifurcation and after the confluence of the microcahnnel. The numerical data was first obtained by using a manual tracking plugin and then analysed by an optimization technique using the genetic algorithm approach. The results show that for the majority of the cases the function that more closely resembles the CFL boundary is the trigonometric function.

Introduction

Blood is a complex fluid composed mainly of suspended red blood cells (RBCs) within plasma where RBCs are responsible for the supply of oxygen and nutrients to the body and removal of carbon dioxide and metabolic wastes from tissues. Throughout the years, several experimental methods were performed in both in vivo [1-4] and in vitro [5-11] environments, in an attempt to understand the flow behavior of RBCs in microchannels and microvessels. These studies have produced significant findings with respect to rheological properties of RBCs. A hemodynamic phenomenon observed in both in vivo and in vitro studies is the formation of a marginal cell-free layer (CFL) at regions adjacent to wall due to the tendency of RBCs to migrate toward the centre

of the microtube [1, 10, 12]. The existence of a cell depleted layer in microvessels, tend to reduce the apparent viscosity of blood and by increasing this layer the blood viscosity tend to decrease in both microchannnels and microvessels. Hence, it is important to understand the behavior of the CFL in microcirculation as it contributes to the rheological properties of blood flowing in microvessels, modulates the nitric oxide scavenging effects by RBCs and may lead to heterogeneous distribution of blood cells in microvascular networks [4, 13].

Although in vivo and vitro experiments give a more realistic information on the flow properties of blood, once validated, physical models and their numerical results are extremely valuable tools to obtain more insight on the blood rheological properties at a micro-scale level. Recently due to the advances of the computational techniques and computing power, several numerical models have been proposed based on a multiphase approach, in which the blood is considered as a multiphase suspension of deformable particles and where levels of submodeling for the blood cells behaviour are also taken into account. Some examples for this type of approach are the boundary element method [14, 15], the immersed boundary method [16, 17], the lattice Boltzmann method [18, 19] the moving particle semi-implicit (MPS) method [20-23] and spring– network model based on the minimum energy concept [24, 25]. Recent reviews on these numerical methods can be found in Liu et al. [26], Yamaguchi et al. [27] and Lima et al. [10]. Although multiphase approaches are promising methods, it is still extremely complex to consider the CFL in their numerical models. The present study tracks RBCs flowing around the CFL and calculates the most suitable function by using global optimization technique. The measurements were performed in a polydimethysiloxane (PDMS) microchannel with a diverging and a converging bifurcation and all images were obtained by means of a high-speed video microscopy system.

The paper is organized as follows. First section shows the materials used in this work and the methods that were applied in this study. The second section presents the numerical results and discussion. The last section presents the main conclusions and some future directions.

Materials and Methods

Microfabrication

Microchannels were initially developed with a CAD software, where the geometries were selected taking into account a previous study about the blood flowing through microchannels with bifurcations and confluences fabricated by a soft lithography technique [9]. The parent microchannels have 300, 500 and 1000 µm in width and the two branches of the bifurcation and confluence corresponds to 50% of the width of parent channel [28]. Illustration 1 shows the configuration of the network and the regions where the CFL was measured.

This geometry was used to fabricate the molds by using a soft xurography technique [28].The mold was used for the production of PDMS microchannels. The PDMS was obtained by mixing a curing agent (10:1 ratio) with PDMS prepolimer. By using of a spin coater, a residual amount of PDMS with a ratio 20:1 was dispersed on a slide glass. The PDMS was cured in an oven at 80 °C for 20 minutes. Then by using a blade the microchannels were cutted off and the inlet/outlet holes of the fluid were done by using a fluid dispensing tip. Finally, to have a strong adhesion of the materials, the device was placed in the oven at 80 °C for 24 hours.

Experimental Set-up

The fabricated microchannels were used to study *in vitro* blood flow with Dextran 40 containing 10% of RBCs. The blood was collected from a healthy sheep and heparin was added to prevent clotting. Additionally, the cells were separated from blood by centrifugation.

A syringe pump (*Harvard Apparatus PHD ULTRA™*) was used to control the flow rate of the working fluid. To visualize and measure the flow we have used an inverted microscope (*IX71, Olympus*) combined with a high speed camera (*i-SPEED LT*). Illustration 2 shows the experimental apparatus used to control the flow and to visualize the CFL within the microchannels. The microfluidic device containing the microchannels was placed on the stage of the inverted microscope and a pressure-driven flow was kept constant by means of a syringe pump. All images have a resolution of 800x600 pixels and were recorded at a frame rate of 200 frames/s.

Image Analysis

A manual tracking plugin (MTrackJ), of the image analysis software Image J, was used to track individual RBC flowing around the boundary of the RBCs core. By using MTrackJ plugin, the centroid of the selected RBC was automatically computed. After obtaining *x* and *y* coordinates of the RBC centroids, the data were exported for the determination of each individual RBC trajectory [5]. Illustration 3 shows a trajectory of a RBC flowing around the boundary region between the CFL and RBCs core.

Global optimization method: Genetic Algorithm

Genetic algorithms are based on theory of evolution of species from Darwin. This method allows to find a global minimum in a large search space [29]. The genetic algorithm starts with a set of solutions called population, where the solution is represented by an individual and the population size is preserved through each generation. The objective function is evaluated in each individual. Then individuals are selected according to their objective value. Those selected will be reproduced up randomly, by using genetic operators such as mutation and crossover. Individuals with less values have a high probability of being selected whereas the new generation of individuals may have a minor objective value than the previous generation. The evolution process is repeated until the stopping criterion is satisfied [30, 31]. By using this method, RBC trajectories obtained are approximated and most suitable function is found out.

Results and Discussion

All videos captured were recorded in four different regions, i. e., region 1 and 3 correspond to locations before the bifurcation whereas region 2 and 4 correspond to locations after the confluence (see illustration 1). Moreover, this study was investigated the CFL behaviour in three kinds of parent microchannels having widths of 300, 500 and 1000 µm. For all the cases, the flow rate was constant (10µl/min) and the working fluid had always a haematocrit of 10%, i. e., containing 10% of ovine RBCs in the solution.

A manual tracking plugin from Image J was used to track individual RBC flowing around the boundary region between the CFL and RBCs core. All the selected RBCs have enough good quality images to track the trajectory of the cells flowing nearby the RBCs core (see Illustration 3). Ilustration 4 shows representative RBC trajectories in the different cases under study, i. e., parent microchannels with widths of 300, 500 and 1000 µm at two different regions (region before the bifurcation and after the confluence).

To obtain the numerical data a nonlinear least squares theory was used. In each region R_{Aw}, R_{Bw}, R_{Cw}, and R_{Dw} for w = 300, 500 and 1000, we have applied the nonlinear optimization problem defined in illustration 5.

After developing a MatLab code and by applying the

genetic algorithm to solve the optimization problem (1), it was possible to obtain the numerical results shown in Table 1. Since the genetic algorithm is a stochastic method, each problem was solved 100 times. Table 1 presents the regions where the problem (1) was applied, the average of the optimum value and the minimum value obtained in the all 100 runs. The table shows that the minimum value for most of the cases corresponds to the function g_3.

Illustration 6 shows an example of two RBCs trajectories flowing in region R_{A500} and R_{B500}, in a parent microchannel with a width of 500 µm, as well as the functions that have revealed a better approximation to the RBCs trajectories. Function g_1 was not displayed mainly because it was the worst approximation solution to the cells trajectories. Overall, the numerical results suggest that the trigonometric function (g_3) is the one that better resembles the RBCs trajectories and consequently the CFL boundaries, since for the majority of the cases studied the minimum value was obtained for this function. The trigonometric function (g_3) may be due to oscillations caused by collisions between neighbourhood cells flowing around the RBCs core. The only exception was verified in the regions $R_{A500,}$ R_{A1000} and R_{B300} , wherein these regions the best fit was obtained with the function . Additionally, these results also show that the CFL boundary is size independent and its flow behaviour is not affected by complex geometries such bifurcations and confluences.

Conclusions and Future Directions

In this study, we present a method to measure individual RBCs trajectories flowing around the CFL region. These cells trajectories are believed to closely resemble the CFL boundary and they were fitted using three different functions. A genetic algorithm was used to solve the constrained optimization problem and the best fit was obtained by using the function (), i.e., a sum of trigonometric functions. As a future work, we will test other functions and examine a bigger variety of physiological fluids used *in vitro* blood studies.

Acknowledgment

The authors acknowledge the financial support provided by: PTDC/SAU-BEB/108728/2008, PTDC/SAU-BEB/105650/2008, and PTDC/SAU-ENB/116929/2010 from FCT (Science and Technology Foundation), COMPETE, QREN and European Union (FEDER).

References

1. Maeda, N. (1996) Erythrocyte rheology in microcirculation. Japanese Journal of Physiology 46: 1-14.

2. Pries, A., Secomb, T. (1994), Resistance to blood flow in microvessels in vivo. Circulation Research 75: 904–915.

3. Suzuki, Y., Tateishi, N., Soutani M. and N., Maeda (1996) Deformation of erythrocytes in microvessels and glass capillaries: effects of erythrocyte deformability. Microcirculation 3: 49-57.

4. Kim S, Kai Ong P, Yalcin O, Intaglietta M, Johnson PC (2009). The cell-free layer in microvascular blood flow. Biorheology 46 (3): 181-189.

5. Lima R, Ishikawa T, Imai Y, Takeda M, Wada S, Yamaguchi T (2008). Radial dispersion of red blood cells in blood flowing through glass capillaries: role of heamatocrit and geometry. J Biomech 44, 2188-2196.

6. Goldsmith, H., Turitto, V. (1986) Rheological aspects of thrombosis and haemostasis: basic principles and applications. ICTH-Report-Subcommittee on Rheology of the International Committee on Thrombosis and Haemostasis. Thromb Haemost. 55: 415–435.

7. Lima, R., Wada, S., et al. (2006) Confocal micro-PIV measurements of three dimensional profiles of cell suspension flow in a square microchannel. Meas. Sci. Tech. 17: 797-808.

8. Lima, R., Ishikawa, T., et al. (2009) Measurement of individual red blood cell motions under high hematocrit conditions using a confocal micro-PTV system. Annals of Biomedical Engineering 37: 1546-1559.

9. Leble V, Lima R, Dias R, Fernandes C, Ishikawa T, Imai Y, Yamaguchi T (2011). Asymmetry of red blood cell motions in a microchannel with a diverging and converging bifurcation. Biomicrofluidics 5, 044120.

10. Lima R, Ishikawa T, Imai Y, Yamaguchi T (2012a). Blood flow behavior in microchannels: advances and future trends. Single and two-Phase Flows on Chemical and Biomedical Engineering, Ricardo Dias, Antonio A. Martins, Rui Lima and Teresa M. Mata (Eds), Bentham Science, 513-547.

11. Garcia V, Dias R, Lima R (2012). In vitro blood flow behaviour in microchannels with simple and complex geometries. Applied Biological Engineering – Principles and Practice, Dr. Ganesh R. Naik (Ed.), ISBN: 978-953-51-0412-4, InTech, 393-416.

12.C. Caro, T. Pedley, R. Schroter, W. Seed, The mechanics of the circulation, Oxford University Press, 1978.

13. Fedosov DA, Caswell B, Popel AS, Karniadakis G (2010). Blood Flow and Cell-Free Layer in Microvessels. Microcirculation 17(8), 615–628.
14. Pozrikidis, C.; Numerical simulation of the flow-induced deformation of red blood cells. Ann. Biomed. Eng. 31, 1194–1205, 2003.
15. Omori T, et al.; Comparison between spring network models and continuum constitutive laws: Application to the large deformation of a capsule in shear flow. Physical Review E, 83, 2011
16. Eggleton, C.D., and Popel, A.S., (1998) Large deformation of red blood cell ghosts in a simple shear flow. Phys. Fluids. 10: 1834–1845.
17. Bagchi, P., Mesoscale simulation of blood flow in small vessels. Biophys. J. 92: 1858–1877, 2007.
18. Succi, S., (2001) The lattice Boltzmann equation for fluid mechanics and beyond, Clarendon Press, Oxford.
19. Dupin, M.M., Halliday, et al. (2007) Modeling the flow of dense suspensions of deformable particles in three dimensions, Phys. Rev. E. 75: 066707.
20. Tsubota, K., e tal., A Particle Method for Blood Flow Simulation – Application to Flowing Red Blood Cells and Platelets, Journal of the Earth Simulator, 5, 2–7, 2006.
21. Tsubota, K., et al., (2006) Particle method for computer simulation of red blood cell motion in blood flow. Computer Methods and Programs in Biomedicine 83: 139-146.
22. Kondo, Y. Imai et al. (2009) Hemodynamic analysis of microcirculation in malaria infection. Annals of Biomedical Engineering 37: 702-709.
23. Imai Y, Kondo H, Ishikawa T, et al. Modeling of hemodynamics arising from malaria infection. J Biomech 2010; 43: 1386-93.
24.Lima R, Nakamura M, Omori T, Ishikawa T, Wada S, Yamaguchi T. Microscale flow dynamics of red blood cells in microchannels: an experimental and numerical analysis, In: Tavares JM, Jorge RM, Eds. Computational Vision and Medical Processing: Recent Trends. Springer, 203-220, 2009.
25. Nakamura M., Bessho S., Wada S., Spring?network?based model of a red blood cell for simulating mesoscopic blood flow, International Journal for Numerical Methods in Biomedical Engineering, 29, 114-128, 2013.
26.Liu, W.K., Liu, Y., et al. (2006) Immersed finite element method and its applications to biological systems. Comput. Methods Appl. Engrg. 195: 1722–1749.
27. Yamaguchi, T., Ishikawa, T., et al., (2006) Computational blood flow analysis – new trends and methods. Journal of Biomechanical Science and Enginneering 1: 29-50.
28. Pinto, E., Pinho, D., Bento, D., et al. 5th Portuguese Congress on Biomechanics, pp. 301- 306, 2013.
29. J. H. Holland,Adaptation in Natural and Artificial Systems, Ann Arbor, The University of MichiAGn Press, 1975.
30.M. Kumar, M.Husian, N. Upreti, D. Gupta, Genetic Algorithm: Review and Application, International Journal of Information Technology and Knowledge Management, 2(2), pp. 451-454, 2010.
31. Catlin, G., Advani, S., Prasad, A. (2011). Optimization of polymer electrolyte membrane fuel cell channels using a genetic algorithm. Journal of Power Sources, 196:9407_9418.

Downloaded from http://www.webmedcentral.com on 29-Aug-2013, 04:29:38 AM

Illustrations

Illustration 1

Schematic representation of the microchannel geometry and location of the sections where the images were collected and the CFL was measured.

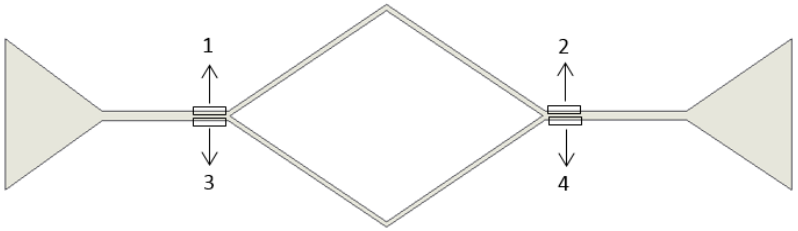

1 – Region A ($R_{A(width)}$);

2 – Region B ($R_{B(width)}$);

3 – Region C ($R_{C(width)}$);

4 – Region D ($R_{D(width)}$);

Downloaded from http://www.webmedcentral.com on 29-Aug-2013, 04:29:38 AM

Illustration 2

Experimental apparatus to control and visualize the flow in microchannels produced by xurography.

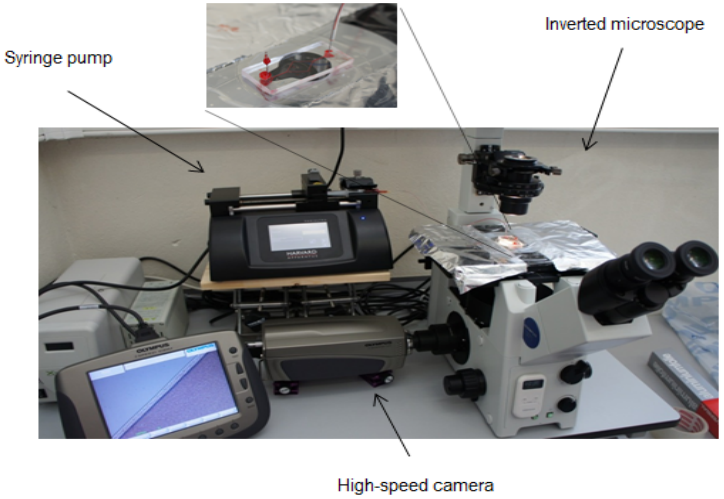

Downloaded from http://www.webmedcentral.com on 29-Aug-2013, 04:29:38 AM

Illustration 3

A trajectory of a RBC flowing around the boundary region between the CFL and RBCs core.

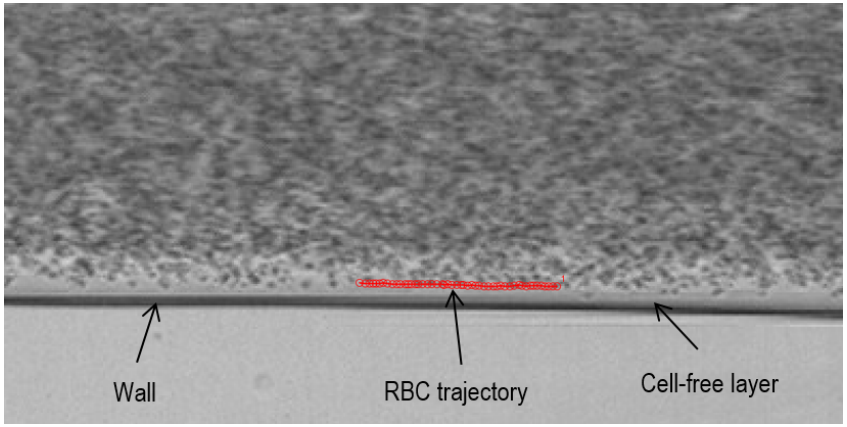

Downloaded from http://www.webmedcentral.com on 29-Aug-2013, 04:29:38 AM

Illustration 4

Trajectories of individual RBCs flowing around the CFL.

a) in region A at parent microchannel of 300 μm; b) in region B at parent microchannel of 300 μm; c) in region A at parent microchannel of 500 μm; d) in region B at parent microchannel of 500 μm; e) in region A at parent microchannel of 1000 μm; f) in region B at parent microchannel of 1000 μm; g) in region C at parent microchannel of 300 μm; h) in region D at parent microchannel of 300 μm; i) in region C at parent microchannel of 500 μm; j) in region D at parent microchannel of 500 μm; k) in region C at parent microchannel of 1000 μm; l) in region D at parent microchannel of 1000 μm.

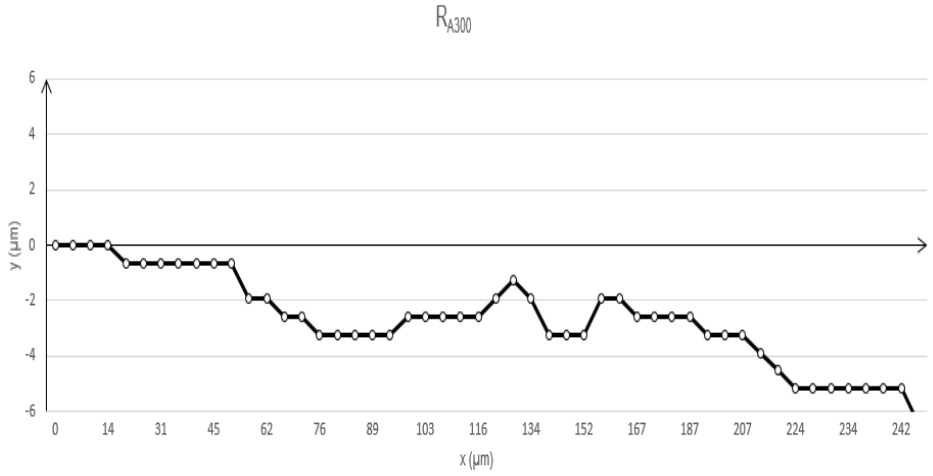

a)

Downloaded from http://www.webmedcentral.com on 29-Aug-2013, 04:29:38 AM

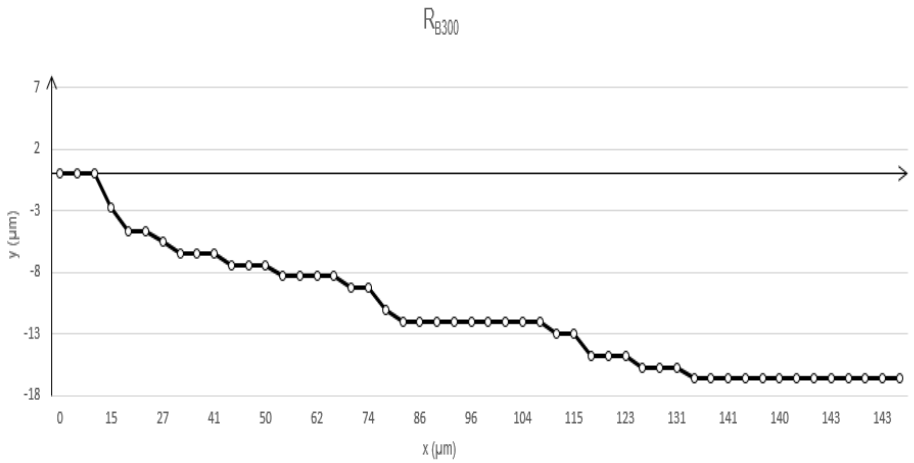

b)

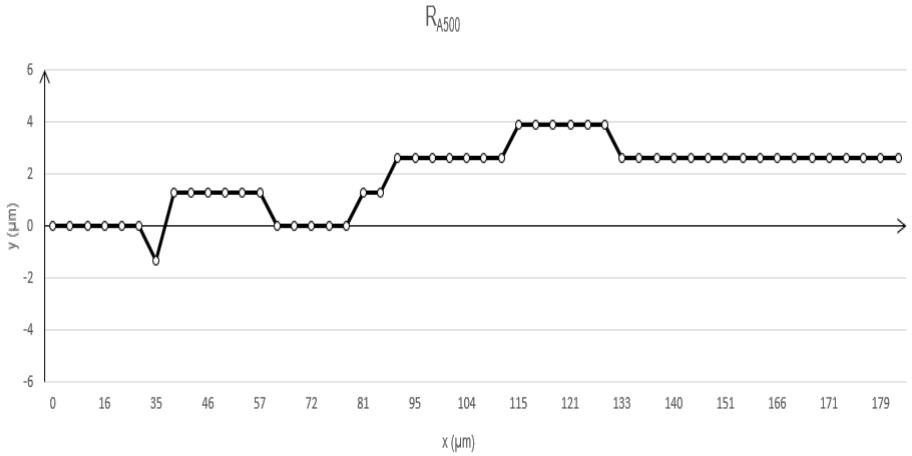

c)

Downloaded from http://www.webmedcentral.com on 29-Aug-2013, 04:29:38 AM

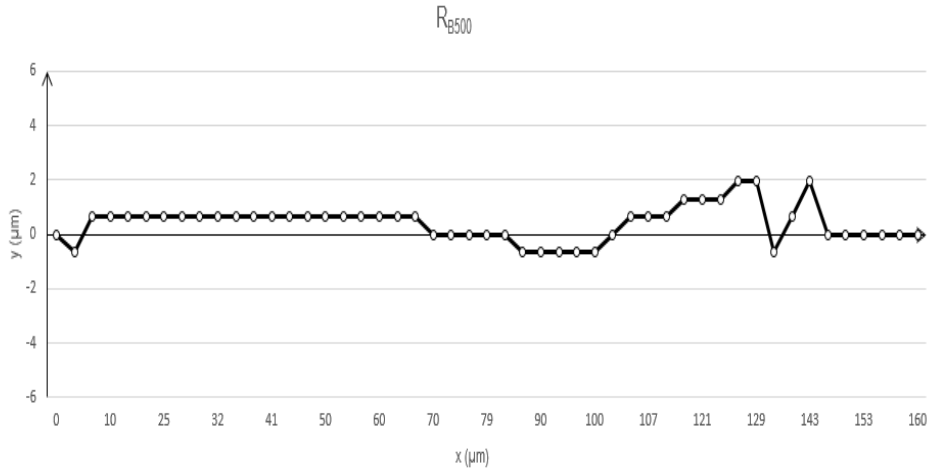

d)

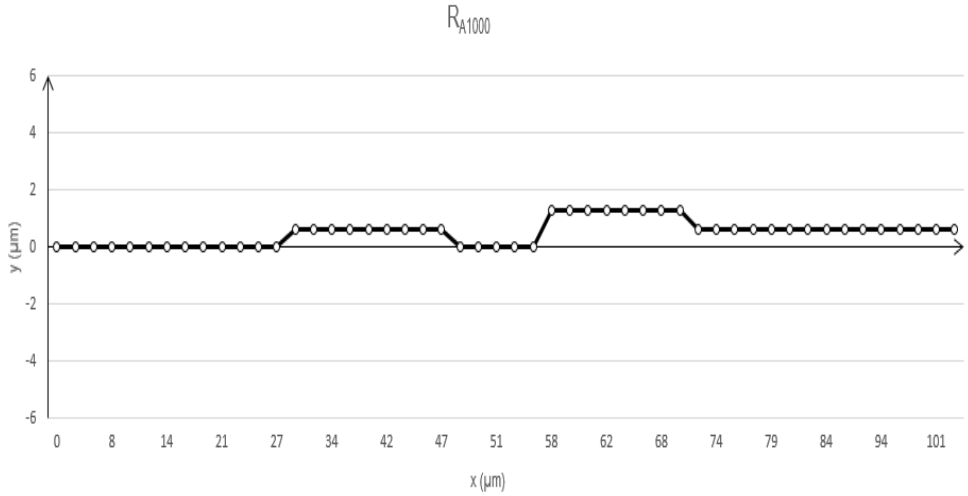

e)

Downloaded from http://www.webmedcentral.com on 29-Aug-2013, 04:29:38 AM

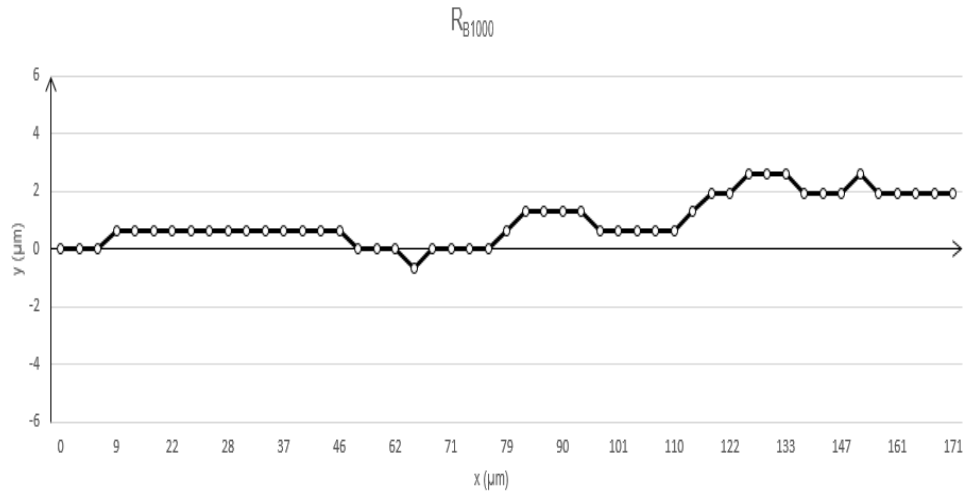

f)

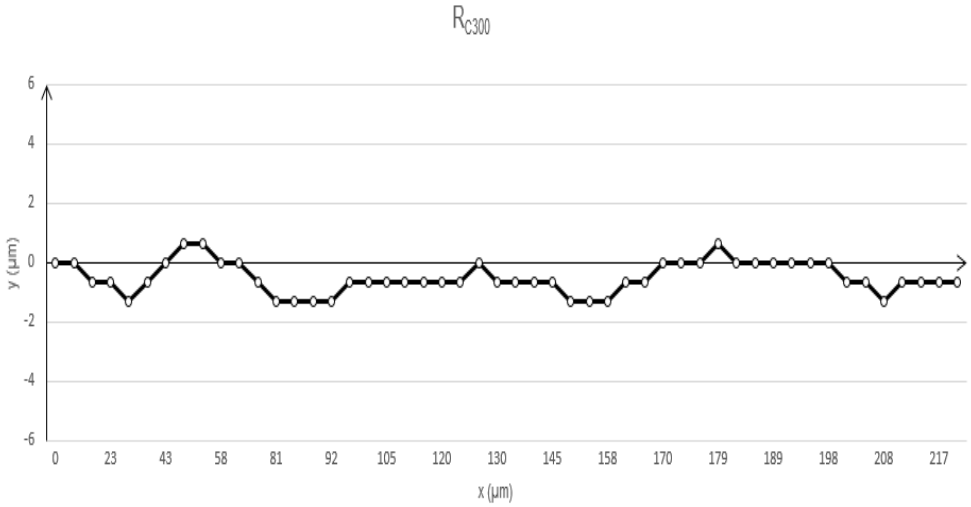

g)

Downloaded from http://www.webmedcentral.com on 29-Aug-2013, 04:29:38 AM

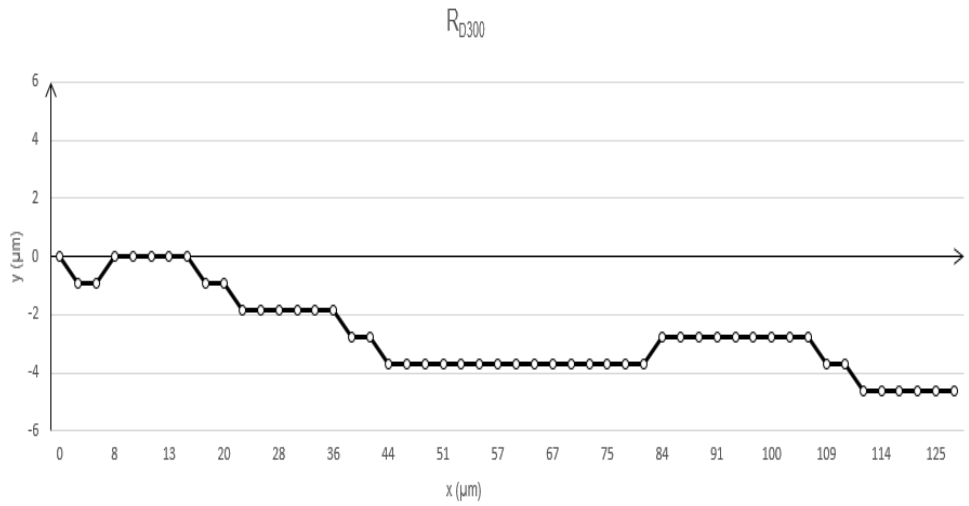

h)

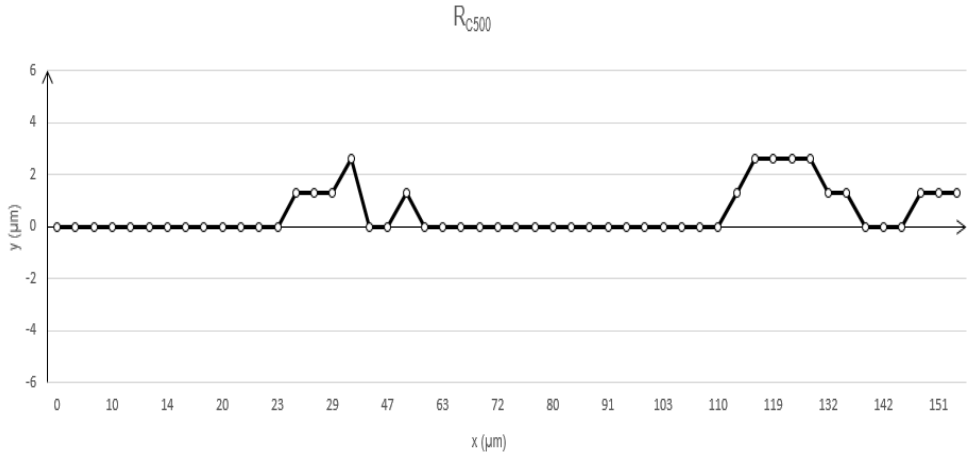

i)

Downloaded from http://www.webmedcentral.com on 29-Aug-2013, 04:29:38 AM

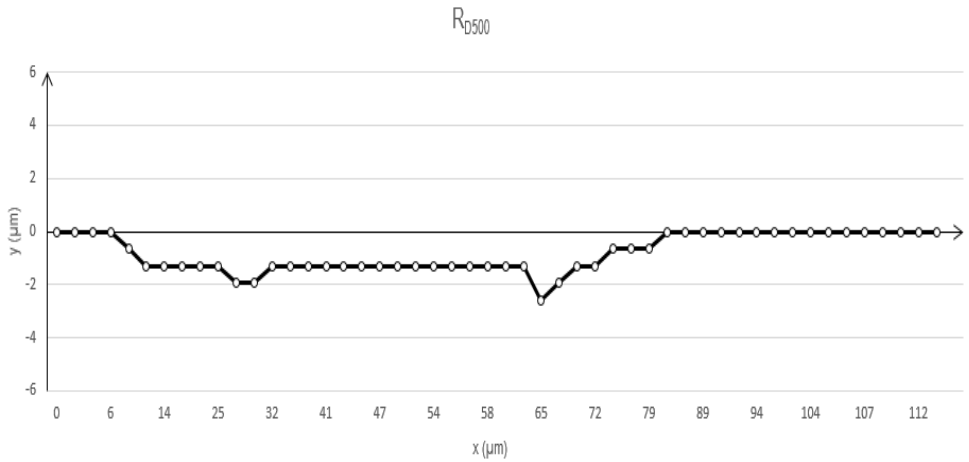

j)

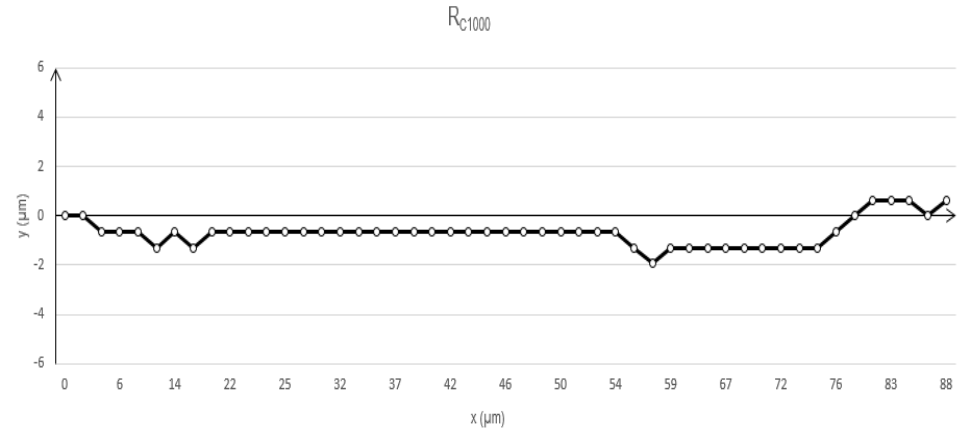

k)

Downloaded from http://www.webmedcentral.com on 29-Aug-2013, 04:29:38 AM

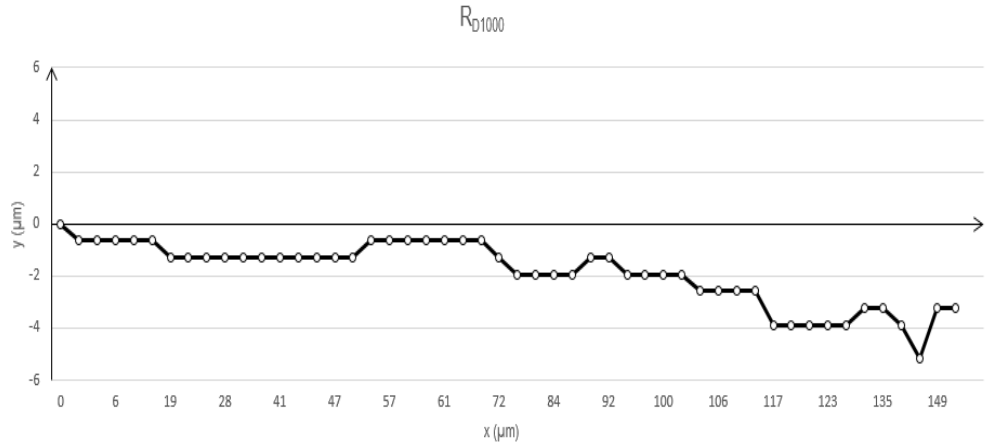

l)

Downloaded from http://www.webmedcentral.com on 29-Aug-2013, 04:29:38 AM

Illustration 5

To obtain the numerical data a nonlinear least squares theory was used. In each region RAw, RBw, RCw, and RDw for w = 300, 500 and 1000, we have applied the nonlinear optimization problem defined as:

$$\min f(y) \equiv \sum_{k=1}^{N_R} (M_k - g_h(y, x_k))^2 \quad (1)$$

$$\text{s.t} \quad g_h(y, x_k) \geq 0 \; \forall k = 1, \ldots, N_R$$

where (,), for $k = 1,\ldots,N_R$ are the CFL measurement of region *R* (defined as R_{Aw}, R_{Bw}, R_{Cw}, and R_{Dw} for *w* = 300, 500 and 1000). The function , for *h*= 1,…,3, are defined as follows:

$$\begin{aligned} g_1(y, x) &= y_1 x^2 + y_2 x + y_3, \\ g_2(y, x) &= y_1 x + y_2, \\ g_3(y, x) &= \sin(y_1 x) + \cos(y_2 x) + y_3. \end{aligned} \quad (2)$$

Downloaded from http://www.webmedcentral.com on 29-Aug-2013, 04:29:38 AM

Illustration 6

RBCs trajectories flowing in region RA500 and RB500, in a parent microchannel with a width of 500 µm, as well as thefunctions that have showed a better approximation.

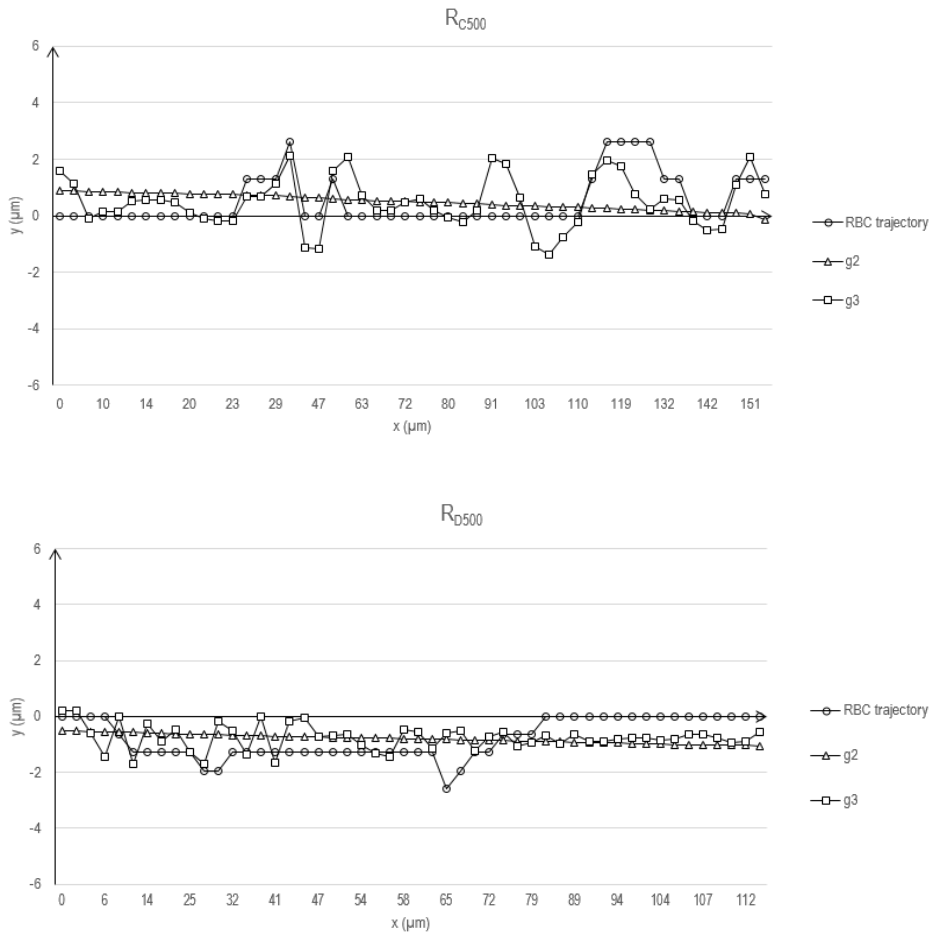

Downloaded from http://www.webmedcentral.com on 29-Aug-2013, 04:29:38 AM

Illustration 7

Numerical results obtained using a genetic algorithm.

Region	Function	Average	Minimun
R_{A300}	g_1	4,90E+05	52,18
	g_2	7,54E+01	31,90
	g_3	**7,39E+01**	**26,89**
R_{A500}	g_1	1,29E+05	59,82
	g_2	**6,24E+01**	**38,76**
	g_3	7,00E+01	45,07
R_{A1000}	g_1	2,00E+04	20,98
	g_2	**1,23E+01**	**6,46**
	g_3	2,09E+01	8,89
R_{B300}	g_1	8,94E+04	97,17
	g_2	**6,93E+01**	**30,42**
	g_3	7,86E+02	621,43
R_{B500}	g_1	1,37E+05	54,71
	g_2	3,99E+01	20,63
	g_3	**3,25E+01**	**19,64**
R_{B1000}	g_1	1,58E+05	50,98
	g_2	2,73E+01	14,33
	g_3	**3,24E+01**	**11,09**

Downloaded from http://www.webmedcentral.com on 29-Aug-2013, 04:29:38 AM

R_{C300}	g_1	2,89E+05	42,35
	g_2	4,88E+01	13,86
	g_3	**2,45E+01**	**10,50**
R_{C500}	g_1	7,30E+04	57,04
	g_2	4,66E+01	32,60
	g_3	**3,93E+01**	**26,63**
R_{C1000}	g_1	1,37E+04	11,36
	g_2	2,16E+01	14,82
	g_3	**2,06E+01**	**6,42**
R_{D300}	g_1	4,20E+04	31,76
	g_2	5,42E+01	35,33
	g_3	**5,23E+01**	**14,36**
R_{D500}	g_1	2,87E+04	13,32
	g_2	2,96E+01	19,96
	g_3	**2,18E+01**	**6,78**
R_{D1000}	g_1	6,92E+04	58,85
	g_2	4,32E+01	18,71
	g_3	**3,50E+01**	**13,60**

Disclaimer

This article has been downloaded from WebmedCentral. With our unique author driven post publication peer review, contents posted on this web portal do not undergo any prepublication peer or editorial review. It is completely the responsibility of the authors to ensure not only scientific and ethical standards of the manuscript but also its grammatical accuracy. Authors must ensure that they obtain all the necessary permissions before submitting any information that requires obtaining a consent or approval from a third party. Authors should also ensure not to submit any information which they do not have the copyright of or of which they have transferred the copyrights to a third party.

Contents on WebmedCentral are purely for biomedical researchers and scientists. They are not meant to cater to the needs of an individual patient. The web portal or any content(s) therein is neither designed to support, nor replace, the relationship that exists between a patient/site visitor and his/her physician. Your use of the WebmedCentral site and its contents is entirely at your own risk. We do not take any responsibility for any harm that you may suffer or inflict on a third person by following the contents of this website.